Journal of Alloys and Compounds 489 (2010) 375–378

Contents lists available at ScienceDirect

Journal of Alloys and Compounds

journal homepage: www.elsevier.com/locate/jallcom

# Hydrogen sorption properties of a Mg–Y–Ti alloy

Claudia Zlotea[a,*,1], Martin Sahlberg[b], Pietro Moretto[a], Yvonne Andersson[b]

[a] Institute for Energy, European Commission, Joint Research Center, P.O. Box 2, NL-1755 Petten, The Netherlands
[b] Materials Chemistry Department, Ångström Laboratory, Uppsala University, Box 538, 751 21 Uppsala, Sweden

ARTICLE INFO

*Article history:*
Received 20 July 2009
Received in revised form 6 September 2009
Accepted 7 September 2009
Available online 23 September 2009

*Keywords:*
Hydrogen storage
Intermetallics
Alloys
Phase transformation

ABSTRACT

The catalytic effect of titanium on the hydrogen sorption properties of a Mg–Y–Ti alloy has been investigated. The alloy is formed by a majority phase $Mg_{24+x}Y_5$, a minor phase of solid solution of Y in Mg and Ti clusters randomly dispersed in the sample. During the first hydrogen absorption cycle 5.6 wt.% hydrogen was absorbed at temperatures above 613 K. The alloy decomposed almost completely to $MgH_2$ and $YH_3$. After hydrogen desorption pure Mg and $YH_2$ were formed. For further absorption/desorption cycles the material had a reversible hydrogen capacity of 4.8 wt.%. The $MgH_2$ decomposition enthalpy was determined to −68 kJ/mol $H_2$, and the calculated activation energy of hydrogen desorption of $MgH_2$ was 150(±10) kJ/mol.



## 1. Introduction

Mg-based materials have been the object of intensive research due to their promising hydrogen storage properties [1,2]. $MgH_2$ has a reversible hydrogen storage capacity of 7.6 wt.%. However, pure Mg shows drawbacks for the use in sustainable storage devices, such as very slow kinetics and poor thermodynamics. In order to overcome these limitations two pathways have been developed. First, the sorption kinetic has been showed to be improved by reducing the Mg particle size by mechanical milling and adding catalysts [3,4]. Mg-based materials milled with Ti catalysts have proven to have faster sorption kinetics as compared to pure Mg [2,4]. The thermodynamics is not changed by milling, but the activation energy of desorption for $MgH_2$ can be reduced. Secondly, Mg can be thermodynamically destabilized by alloying with other elements. For example, $Mg_2NiH_4$ has improved thermodynamic and kinetic properties on the expenses of the total capacity [5]. Along with thermodynamic changes, alloying can also improve the hydrogen diffusion properties. Our previous study on solid solution $Mg_{1-x}Y_x$ ($x$ = 0–0.17) thin films has demonstrated improved hydrogen diffusion [6].

Recently, we have discovered that one-dimensional nanostructures of $MgH_2$ can be produced by hydrogenation and subsequent decomposition of the intermetallic compound $Mg_{24}Y_5$ [7]. Hydrogen desorption from one-dimensional $MgH_2$ nanostructures produced carved tubes of pure Mg with nano-sized walls [8]. The elements Y and Ti have previously proven to have an important effect on hydrogen sorption kinetics of Mg-based materials. However, the Mg–Y–Ti ternary phase diagram has received little attention and to our knowledge, no previous report has been published. In the present study, structural, microstructural and hydrogen sorption properties of a bulk Mg–14.5 at%Y–0.5 at%Ti ternary alloy are presented and discussed.

## 2. Experimental details

### 2.1. Synthesis

A Mg-rich alloy with 14.5 at%Y and 0.5 at%Ti was prepared from appropriate amounts of the elements. In order to avoid Mg evaporation and contamination, the pure metals were sealed inside a Ta crucible under Ar atmosphere. The tantalum tubes were heated up to 1073 K in a high frequency induction furnace filled with 30 kPa Ar. No reaction between the tantalum tube and the sample could be observed. The sample was kept and handled inside a glove box under Ar atmosphere.

### 2.2. Structural and microstructural characterizations

Structural and microstructural characterizations were performed by X-rays diffraction (XRD) and scanning electron microscopy (SEM). The XRD experiments were carried out on a Bruker D8 equipped with a Våntec position sensitive detector and a Philips diffractometer with Bragg–Brentano geometry both with Cu $K\alpha_1$ radiation. The lattice parameters were refined using the UNITCELL software (©BeN Systems, 2000). Silicon was used as internal calibration standard.

The microstructural and elemental investigations were performed in a high resolution LEO Supra 50 scanning electron microscope equipped with an in-lens detector and an energy dispersion detector (EDS). The specimens were prepared either by polishing a bulk piece of the pristine sample or by dispersing the powder material (after hydrogen absorption and desorption) on a carbon tape.

### 2.3. Pressure–composition–isotherm and thermal desorption spectroscopy measurements

Pressure–composition–isotherms (PCI) and thermal desorption spectroscopy (TDS) were performed in a volumetric instrument (Hiden Isochema) designed for

* Corresponding author.
*E-mail address:* claudia.zlotea@gmail.com (C. Zlotea).
[1] Now at: IMCPE, CNRS, Thiais, France.

0925-8388/$ – see front matter © 2009 Elsevier B.V. All rights reserved.
doi:10.1016/j.jallcom.2009.09.085

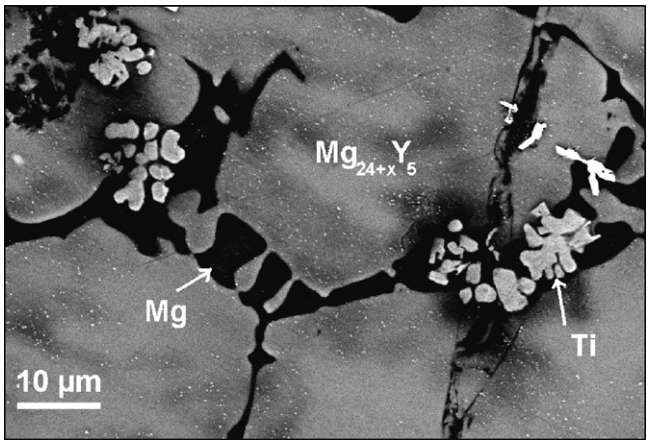


**Fig. 1.** Backscattered electron image of the Mg–Y–Ti alloy. The chemical composition of each phase, as determined by EDS, is indicated.

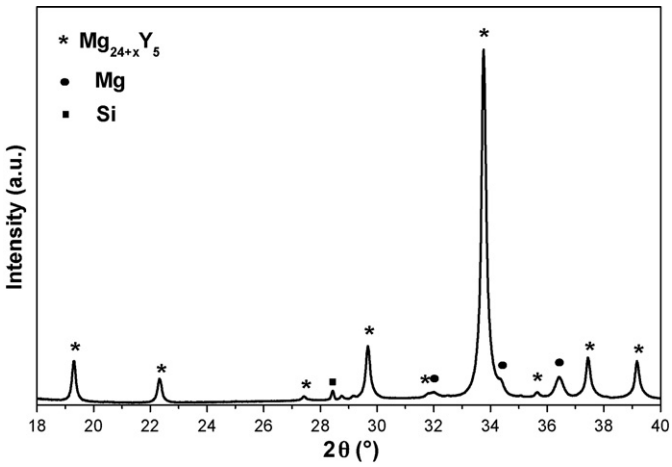


**Fig. 2.** XRD pattern of the Mg–Y–Ti alloy. The diffraction peaks of the $Mg_{24+x}Y_5$ and Mg phases are also indicated. Si is used as internal calibration standard.

measurements of hydrogen absorption/desorption isotherms and the total amount of the thermally desorbed hydrogen. The reactor is equipped with a cryo-furnace (77–773 K) and the volumes of dosing and reactor chambers are approximately 5 $cm^3$. The reactor is connected to a high sensitivity dynamic sampling mass spectrometer by a flexible quartz capillary. Prior to measurements, the reactor was evacuated to a base pressure of $10^{-2}$ Pa and flushed several times with hydrogen and/or helium gases.

The PCI measurements were recorded by the static volumetric method (Sieverts method) by a step-wise increase/decrease of the hydrogen pressure. The maximum hydrogen pressure and temperature are 8 MPa and 673 K, respectively. Prior to the PCI measurements, a gas leak test was performed at high pressure for several hours at room temperature. Thermal gradient corrections and the real equation of state for hydrogen are applied for the calculation of the hydrogen uptake [9]. The thermal stability during the isothermal measurements is ±0.3 K. All PCI curves are confirmed by a second measurement in a similar volumetric instrument with comparable results.

The hydrogen was thermally desorbed in a constant helium flow of 100 ml/min and 100 kPa by heating the sample with a linear temperature rate. The desorbed hydrogen was measured as the hydrogen partial pressure of the mass spectrometer in function of time.

## 3. Results and discussion

### 3.1. The Mg–Y–Ti alloy

The SEM investigations proved that no ternary alloy had been formed, as seen in Fig. 1. Magnesium-rich $Mg_{24+x}Y_5$ ($x = 5.5$) was the majority phase. Second and third phases were identified as Mg-rich with Y in a solid solution and small grains of pure Ti, respectively. The Y content in the Mg solid solution could not be reliably estimated from EDS due to the small amount. Ti dendritic particles, with thicknesses of several tens of micrometers, were randomly distributed in the sample. According to these results Ti did not react with the other elements during melting.

The XRD pattern (Fig. 2) showed that the sample contained $Mg_{24+x}Y_5$ as the main phase and a small fraction of Mg. The small amount of Ti, 0.5 at%, was not possible to be detected in the powder diffraction profiles.

The lattice parameter of $Mg_{24+x}Y_5$, space group $I\bar{4}3m$, was determined to $a = 11.2584(5)$ Å, which was in good agreement with previous studies of the homogeneity range of $Mg_{24+x}Y_5$ [10,11].

The unit cell parameters of hexagonal Mg were determined to $a = 3.2293(3)$ Å and $c = 5.2167(4)$ Å, which were larger than elemental Mg, $a = 3.209$ Å and $c = 5.211$ Å [12] indicating a solid solution of Y in Mg. The solid solubility was estimated to 3.3 at%, from Vegard's law by the use of the unit cell volumes of elemental Mg and Y [12,13]. The results were in accordance with previous investigations of the Mg–Y phase diagram [10,11].

### 3.2. Structural and microstructural changes by hydrogen absorption and desorption

The Mg–Y–Ti alloy absorbed hydrogen at temperatures above 613 K. Hydrogen desorption occurred in the same temperature range under a continuous He flow of 100 ml/min at 100 kPa. The XRD patterns of hydrogenated sample at 2 MPa and 643 K (bottom) and the corresponding desorbed sample (top) are shown in Fig. 3. The hydrogen absorption at 2 MPa and 643 K induced a dissociation of the initial alloy into $YH_3$ and $MgH_2$. Traces of Mg and $YH_2$ were noticed, which indicated that the sample was not fully hydrogenated under these temperature and pressure conditions. The decomposition of this alloy under hydrogen pressure was in agreement with our previous results obtained for $Mg_{24}Y_5$ [7]. $Mg_{24}Y_5$ reacted irreversibly with hydrogen in two-steps. The first step occurred at a moderate hydrogen pressure (50 kPa) and $YH_2$ and Mg were formed. The second step, at higher hydrogen pressures, promoted the formation of $YH_3$ and $MgH_2$. Hydrogen was thermally released from the two-phase sample by heating at similar temperatures and pure Mg and $YH_2$ were formed. Therefore, hydrogen desorption comprises two desorption reactions: from $MgH_2$ to Mg and from $YH_3$ to $YH_2$. $YH_2$ is a very stable hydride and temperatures above 1063 K are needed to desorb the hydrogen [14].

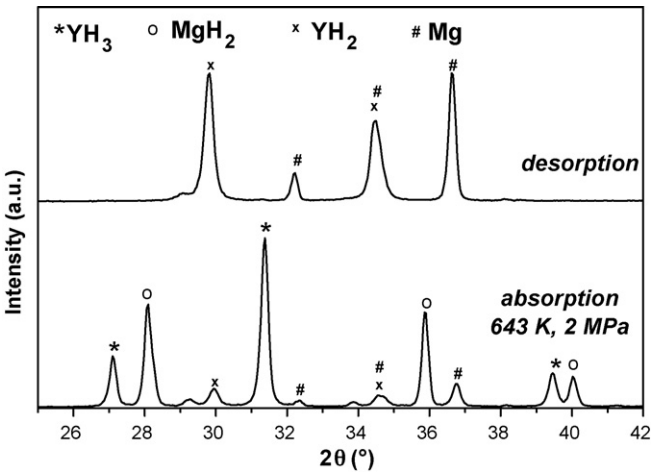


**Fig. 3.** XRD patterns of the Mg–Y–Ti alloy after hydrogen absorption at 2 MPa and 643 K (bottom) and desorption (top).

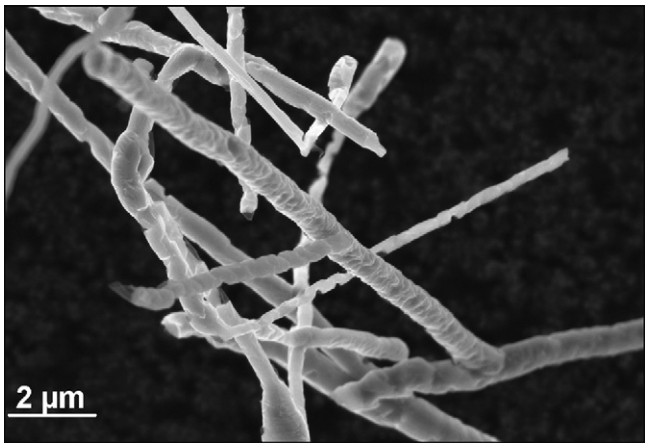


**Fig. 4.** Secondary electrons image of Mg tubes formed by hydrogen desorption from $MgH_2$ whiskers.

One-dimensional structures, in the form of $MgH_2$ whiskers, were grown during hydrogen absorption in the Mg–Y–Ti sample. During hydrogen desorption the whiskers were transformed to one-dimensional Mg carved tubes, as shown by SEM picture, Fig. 4. A similar behavior was previously discovered for hydrogen absorption and desorption in $Mg_{24}Y_5$ [7,8].

### 3.3. Thermodynamic properties of hydrogen sorption

Pressure–composition–isotherm curves, recorded during the first and second hydrogen absorption cycles at 648 K are shown in Fig. 5. The first isotherm absorption curve had a small plateau at a very low pressure, which corresponded to $YH_2$ formation [15,16]. The maximum hydrogen content of this first transition was ~0.8 wt.%, due to the formation of $YH_2$ from all available Y in the sample. A second plateau was obtained at 1.2 MPa hydrogen pressure, due to $MgH_2$ formation. This plateau remained for the second and following cycles. The maximum hydrogen content for the first absorption cycle was 5.6 wt.%, which was slightly lower than the maximum theoretical capacity of 6 wt.% corresponding to the complete hydrogenation of the available Mg and Y to $MgH_2$ and $YH_3$, respectively. For further absorption cycles, the maximum reversible capacity decreased to 4.8 wt.%, since $YH_2$ was stable under these experimental conditions. The reversible hydrogenation reactions were $Mg \leftrightarrow MgH_2$ and $YH_2 \leftrightarrow YH_3$, which was confirmed by XRD results. The phase transition $YH_2 \leftrightarrow YH_3$ was not verified

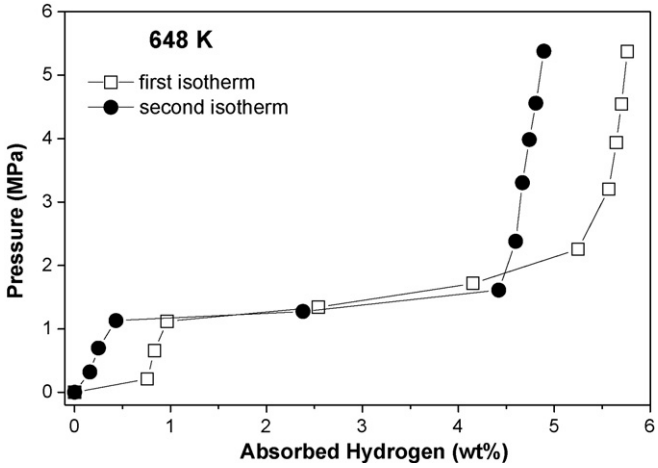


**Fig. 5.** Pressure–composition–isotherms recorded at 648 K for the first and second hydrogen absorption cycles of Mg–Y–Ti.

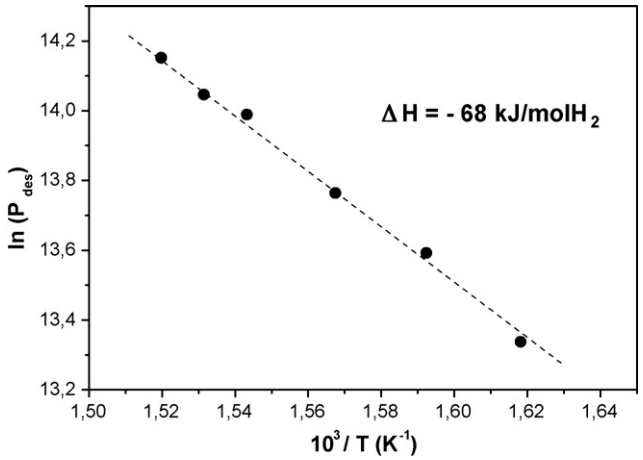


**Fig. 6.** Van't Hoff plot of the hydrogen desorption from hydrogenated Mg–Y–Ti alloy. The calculated enthalpy of desorption is indicated.

in the PCI measurements, probably due to the small amount of involved hydrogen. Therefore, the maximum reversible hydrogen capacity was 4.8 wt.% at temperature 648 K.

Several absorption and desorption PCI curves were measured at temperatures between 618 and 658 K. The enthalpy of hydrogen desorption ($\Delta H$) was calculated for the values of the plateau pressures ($p$) of desorption isotherms as a function of temperature ($T$) using the Van'f Hoff relation:

$$\ln(p) = \frac{\Delta H}{RT} - \frac{\Delta S}{R} \quad (1)$$

where $\Delta S$ is the entropy of reaction and $R$ is the universal gas constant. The enthalpy of desorption was calculated from the slope of the linear interpolation of the Van't Hoff plot (Fig. 6). The correlation coefficient for the linear regression was 0.998. The calculated $\Delta H = -68$ kJ/mol$H_2$ was in good agreement with the previously reported values of $MgH_2$ decomposition [17]. The results showed that the thermodynamic properties of magnesium hydride did not significantly change by the presence of Y and Ti in the pristine Mg–Y–Ti alloy.

### 3.4. Kinetic properties of the hydrogen desorption

The kinetic properties of the hydrogen desorption were studied by thermal desorption spectroscopy. The recorded and normalized TDS spectra from hydrogenated Mg–Y–Ti alloy at different heating rates (0.5–17 K/min) are displayed in Fig. 7. The temperature where the desorption rate reached its maximum, shifts to higher temperatures for faster heating rates. All TDS spectra showed one main peak, which corresponds to hydrogen desorption from $MgH_2$ [18]. The phase transition $YH_3 \rightarrow YH_2$ could not be verified either by TDS or PCI methods.

The activation energy of desorption was calculated according to the Kissinger method by using the temperature of the maximum hydrogen desorption rate, $T_m$, at different linear heating rates, $h$ [19,20]. The Kissinger equation is:

$$\ln\left(\frac{h}{T_m^2}\right) = -\frac{E_a}{RT_m} + \ln k_0 \quad (2)$$

where $E_a$ is the activation energy of desorption and $k_0$ is a reaction constant. The activation energy $E_a$ was calculated from the logarithmic plot of $h/{T_m}^2$ versus $1/T_m$ (Fig. 8). The correlation coefficient for the linear regression was 0.975. The obtained value $E_a = 150(\pm 10)$ kJ/mol, was in good agreement with earlier reported values for $MgH_2$: 160 (10) kJ/mol (by volumetric technique) [21], 142 kJ/mol (by TDS) [18], 161 (15) kJ/mol (by TDS) [22]. Thus, there

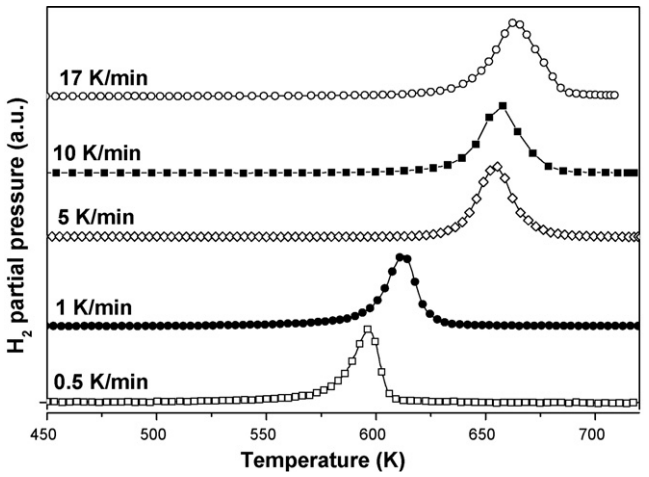


**Fig. 7.** Hydrogen thermal desorption spectra from hydrogenated Mg–Y–Ti alloy recorded at different heating rates.

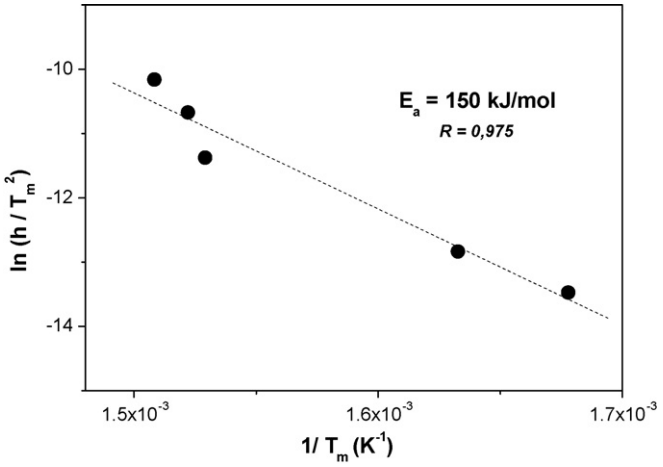


**Fig. 8.** Kissinger plots for the calculation of the activation energy of hydrogen desorption from hydrogenated Mg–Y–Ti.

were no indications for kinetic improvements due to the presence of metallic Ti clusters dispersed within the pristine Mg–Y–Ti alloy.

## 4. Conclusions

Structural, microstructural and hydrogen sorption properties of a Mg–Y–Ti ternary alloy with 85.0 at.% Mg, 14.5 at.% Y and 0.5 at.% Ti composition have been determined by XRD, SEM, PCI and TDS methods. Three phases, $Mg_{24+x}Y_5$ ($x = 5.5$), a solid solution of Y in Mg, and Ti particles, were identified. There were no indications of any reactions with titanium. The alloy absorbed hydrogen at temperatures above 613 K. At 20 MPa hydrogen gas and 643 K the alloy completely decomposes into $YH_3$ and $MgH_2$. Hydrogen was desorbed in a He flow at the same temperature range and the Mg and $YH_2$ phases were formed. Hydrogen was not desorbed from $YH_2$ at this temperature.

The maximum reversible hydrogen capacity was 4.8 wt.% after the second cycle, which was lower than the first cycle capacity 5.6 wt.%. The $MgH_2$ decomposition enthalpy was determined to $-68$ kJ/mol$H_2$, which is in good agreement with previously published values.

The calculated activation energy of hydrogen desorption of $MgH_2$, 150(±10) kJ/mol, in good agreement with decomposition of pure $MgH_2$.

Finally, the presence of both Y and Ti in this Mg-rich alloy did not show any thermodynamic nor kinetic improvement with respect to the hydrogen sorption properties of pure magnesium hydride.

## References

[1] P. Selvam, B. Viswanathan, C.S. Swamy, V. Srinivasan, Magnesium and magnesium alloy hydrides, Int. J. Hydrogen Energy 11 (1986) 169–192.
[2] M. Dornheim, S. Doppiu, G. Barkhordarian, U. Boesenberg, T. Klassen, O. Gutfleisch, R. Bormann, Hydrogen storage in magnesium-based hydrides and hydride composites, Scripta Mater. 56 (2007) 841–846.
[3] A. Zaluska, L. Zaluska, J.O. Ström-Olsen, Structure, catalysis and atomic reactions on the nano-scale: a systematic approach to metal hydrides for hydrogen storage, Appl. Phys. A 72 (2001) 157–165.
[4] G. Liang, J. Huot, S. Boily, A. Van Neste, R. Schulz, Catalytic effect of transition metals on hydrogen sorption in nanocrystalline ball milled $MgH_2$–Tm (Tm = Ti, V, Mn, Fe and Ni) systems, J. Alloys Compd. 292 (1999) 247–252.
[5] J.J. Reilly, R.H. Wiswall, Reaction of hydrogen with alloys of magnesium and nickel and the formation of $Mg_2NiH_4$, Inorg. Chem. 7 (1968) 2254–2256.
[6] C. Chacon, E. Johansson, C. Zlotea, Y. Andersson, B. Hjorvarsson, Growth and hydrogen uptake of Mg–Y thin films, J. Appl. Phys. 97 (2005), 104903, 1–6.
[7] C. Zlotea, J. Lu, Y. Andersson, Formation of one-dimensional $MgH_2$ nanostructures by hydrogen induced disproportionation, J. Alloys Compd. 426 (2006) 357–362.
[8] C. Zlotea, M. Salhberg, S. Özbilen, P. Moretto, Y. Andersson, Hydrogen desorption studies of the Mg24Y5–H system: Formation of Mg tubes, kinetics and cycling effects, Acta Mater. 56 (2008) 2421–2428.
[9] Lemmon EW, Huber ML, Friend DG, Paulina C. Standardized equation for hydrogen gas densities for fuel consumption applications. Contribution of the National Institute of Standards and Technology, 2006-01-0434.
[10] J.F. Smith, D.M. Bailey, D.B. Novotny, J.E. Davison, Thermodynamics of formation of yttrium–magnesium intermediate phases, Acta Metall. 13 (1965) 889–895.
[11] F. Bonhomme, K. Yvon, Synthesis and crystal structure refinement of cubic $Mg_{6.8}Y$, J. Alloys Compd. 232 (1996) 271–273.
[12] Natl. Bur. Stand. (U.S.) Monogr. 25 21 (1985) 82.
[13] Natl. Bur. Stand. (U.S.) Monogr. 25 18 (1981) 77.
[14] V.A. Yartys, O. Gutfleisch, V.V. Panasyuk, I.R. Harris, Desorption characteristics of rare earth (R) hydrides (R = Y, Ce, Pr, Nd, Sm, Gd and Tb) in relation to the HDDR behaviour of R–Fe-based-compounds, J. Alloys Compd. 253–254 (1997) 128–133.
[15] L.N. Yannopoulos, R.K. Edwards, P.G. Wahlbeck, The thermodynamics of the yttrium–hydrogen system, J. Phys. Chem. 69 (1965) 2510–2515.
[16] A.S. Chernikov, V.I. Savin, V.N. Fadeev, N.A. Landin, L.A. Izhvanov, Thermodynamic and physical properties of yttrium and some rare earth hydrides, J. Less Common Metals 130 (1987) 441–452.
[17] F.H. Ellinger, C.E. Holley Jr., B.B. McInteer, D. Pavone, R.M. Potter, E. Staritzky, W.H. Zachariasen, The preparation and some properties of magnesium hydride, J. Am. Chem. Soc. 77 (1955) 2647–2648.
[18] J.S. Han, M. Pezat, J.-Y. Lee, A study of the decomposition of magnesium hydride by thermal analysis, J. Less Common Metals 130 (1987) 395–402.
[19] H.E. Kissinger, Reaction kinetics in differential thermal analysis, Anal. Chem. 29 (1957) 1702–1706.
[20] A.M. de Jong, J.W. Niemantsverdriet, Thermal desorption analysis: comparative test of ten commonly applied procedures, Surf. Sci. 233 (1990) 355–365.
[21] J.F. Fernandez, C.R. Sanchez, Rate determining step in the absorption and desorption of hydrogen by magnesium, J. Alloys Compd. 340 (2002) 189–198.
[22] J.F. Fernandez, C.R. Sanchez, Simultaneous TDS–DSC measurements in magnesium hydride, J. Alloys Compd. 356–357 (2003) 348–352.